Optimized Design of Multilayer Barrier Films Incorporating a Reactive Layer. II. Solute Dynamics in Two-Layer Films

Stanislav E. Solovyov, Anatoliy Y. Goldman

Department of Materials and Processing, Alcoa Closure Systems International, Incorporated, 1205 Elmore Street, Crawfordsville, Indiana 47933

Received 25 October 2004; accepted 30 August 2005
DOI 10.1002/app.23439
Published online 3 February 2006 in Wiley InterScience (www.interscience.wiley.com).

ABSTRACT: Extending the model of transient permeation through the reactive barrier film presented in part I of this series to two-layer reactive–passive barrier structures, we devote part II to the analysis of the evolution of interfacial solute concentrations between the layers. The concepts developed earlier are applied to the transient ingress analysis of two-layer films where one of the layers contains a noncatalytic solute scavenger. In particular, we show that for reactive–passive films, the averaging approximation of the transient interfacial solute concentration provides good agreement with numerical results for the transient effective flux. The applicability range of this averaging and the error introduced by it are quantified. For the passive–reactive films, the same averaging fails to predict the effective flux dynamics. A new method of ingress analysis is presented for such structures to correct the situation. The method is based on the effective flux dynamics in the homogeneous reactive membrane and the dynamic reactive to the passive–reactive flux scaling between the initial and final solute concentration profiles corresponding to the scavenger activation and scavenger exhaustion times. © 2006 Wiley Periodicals, Inc. J Appl Polym Sci 100: 1952–1965, 2006

Key words: permeable; reactive; barrier; membranes

INTRODUCTION

In part I[1] of this series of articles, we presented the analysis methodology for transient solute ingress into a package through single-layer noncatalytic reactive films. In real-world packaging applications, however, the solute scavenger is almost never dispersed throughout the entire film thickness because the byproducts of the scavenging reaction in many cases cannot be put into direct contact with the packaged product. Multilayer passive barrier packaging solutions have become a commonplace, and there are few technological limitations on the placement of the scavenger within any sublayer in the multilayer structure. To gain understanding of how such placement affects the barrier properties of a reactive–passive (RP) layered structure, we first needed to develop the analysis methodology for the simplest two-layer cases of RP and passive–reactive (PR) films (distinguished by the reactive layer placement relative to solute-rich and solute-poor environments separated by a barrier). More complex multilaminar heterogeneous structures containing a reactive layer could then be analyzed to optimize the layer sequence and scavenger placement. Specifically, we were interested in how the scavenger placement in one of the layers relative to the separated environments and the transport properties of the reactive layer matrix in relation to other (passive) layers affected the transient barrier properties of the multilayer structure. The impact of such selection on the optimization of commercial packaging designs containing oxygen scavengers cannot be overestimated.

Another driving force for this research was a desire to provide a quick analytical tool to polymer and packaging engineers that would allow them to compare potential multilayer designs and select the optimal one for a targeted application. This is especially important because the numerical integration of systems of partial differential equations with discontinuous coefficients (layer material diffusivities of a heterogeneous layered structure) requires additional approximations and assumptions to make the problem well posed and yet be able to correctly represent reaction–diffusion dynamics in multilayer barrier structures. The accuracy of such numerical results for ill-posed problems in heterogeneous membranes comprised of many thin layers and with large differences in solute transport properties between the adjacent layers can also be questionable. In part II, we propose an analytical method for such an analysis based on the Solovyov–Goldman (SG) theory of transient permeation,[2–4] including a semipermeable reaction wave-

Correspondence to: S. E. Solovyov, Multisorb Technologies, Incorporated, 325 Harlem Road, Buffalo, NY 14224 (ssolovyov@multisorb.com).

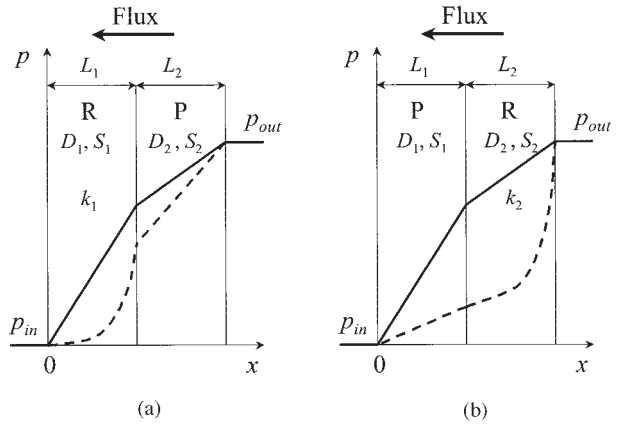

Figure 1 Steady-state solute partial pressure profiles in the (a) RP and (b) PR films with catalytic scavenging reactions in the (- - -) reactive (R) layer. Solid lines represent pressure profiles across the PP film (P = passive layer).

front model and its extension for the analysis of solute ingress into the package. The terminology and notation in part II continue from part I.

TWO-LAYER FILMS WITH A REACTIVE LAYER

RP and PR film designs with different material properties of laminated or coextruded layers are considered, as shown in Figure 1(a,b). The RP film refers to the RP laminate design with the reactive layer (R) exposed to the package contents (with the solute pressure p_{in}) and the passive layer (P) is exposed to the environment ($p_{out} > p_{in}$, where p_{out} is the partial solute pressure outside the package and p_{in} is the partial solute pressure inside the package). The PR film has the opposite sequence of layers; in both cases, the layer materials are numbered from the membrane surface exposed to p_{in} (index 1). For the case of two-layer films, the properties of the layer material exposed to p_{out} have index 2. The SG model of transient permeation[2–4] is able to predict permeation dynamics through such structures if one solves steady-state reaction–diffusion equations for the RP and PR films to determine the initial permeant concentration profiles when the scavenger reactive capacity is not yet affected by the reaction (with an excess of scavenger for the initial permeant profile formation across the RP structure to approximate the catalytic reaction). The initial interfacial concentrations at the reactive and passive sides of the RP interface (C_1 and C_2, respectively) correspond to continuity of the solute partial pressure across the interface: $p_1 = p_2$ or, according to Henry's law generally valid for permanent gases at ambient conditions dissolved in polymer matrices

$$\frac{C_1}{S_1} = \frac{C_2}{S_2} \tag{1}$$

where S_1 and S_2 are the solubility coefficients of a particular solute in the layer 1 and 2 matrices, respectively. Then, for $p_{in} = 0$, these concentrations are found for the RP film as in ref. 3:

$$C_1^{RP} = \frac{C_{out} S_1 D_2 (e^{2\phi_1} - 1)}{(e^{2\phi_1} + 1)(S_2 D_2 + S_1 L_2 \sqrt{k_1 D_1}) - 2 S_2 D_2} = \frac{C_{out} H_{12} (e^{2\phi_1} - 1)}{(e^{2\phi_1} + 1)(H_{12}\Omega_{12} + 1) - 2} \tag{2}$$

$$C_2^{RP} = \frac{S_2}{S_1} C_1^{RP} = \frac{C_{out} S_2 D_2 (e^{2\phi_1} - 1)}{(e^{2\phi_1} + 1)(S_2 D_2 + S_1 L_2 \sqrt{k_1 D_1}) - 2 S_2 D_2} = \frac{C_{out} (e^{2\phi_1} - 1)}{(e^{2\phi_1} + 1)(H_{12}\Omega_{12} + 1) - 2} \tag{3}$$

where C_{out} is the equilibrium concentration of the solute within the outer membrane boundary; D_1 and D_2 are the solute diffusivities in layers 1 and 2, respectively; ϕ_1 denotes the initial Thiele modulus ϕ_{01} for the fully activated reactive layer 1 in the RP film; L_2 is the thickness of layer 2; k_1 (= $\mu K_1 R_0$, where μ is the stoichiometric reactive capacity of the scavenger, K_1 is the reaction rate constant in layer 1, and R_0 is the initial concentration of the scavenger in the film material) is the initial apparent pseudo-first-order reaction rate in reactive layer 1; Ω is the coupling parameter; and H_{12} is the solute partition coefficient between the layers and is obtained from the solubility coefficients with eq. (1) and with the assumption of Henry's law:

$$H_{12} = \frac{S_1}{S_2} \tag{4}$$

Ω_{12}, representing a synergistic effect of the reactive and passive layer properties on solute transport through the heterogeneous structure, is

$$\Omega_{12} = L_2 \frac{\sqrt{k_1 D_1}}{D_2} = L_1 \sqrt{\frac{k_1}{D_1}} \left[\frac{D_1}{L_1} \frac{L_2}{D_2} \right] = \phi_1 \zeta_{1R2P} \tag{5}$$

where L_1 is the thickness of layer 1 and the dimensionless parameter ζ_{1R2P} is defined as a ratio:

$$\zeta_{1R2P} = \left(\frac{D_1}{L_1} \right)_R \Big/ \left(\frac{D_2}{L_2} \right)_P \tag{6}$$

ζ_{1R2P} represents a ratio of the kinetic transport properties of the passive matrix of layer 1 to those of layer 2 where layer 1 contains a scavenger and is initially reactive. By default, layer 1 is always exposed to the package contents with $p_{in} < p_{out}$. Hence ζ_{1R2P} expresses the relative passive barrier performance of the

reactive layer matrix protected from the dominating solute flux direction by a passive layer.

For the PR film, the interfacial concentrations are obtained as follows:[3]

$$C_1^{PR} = \frac{2C_{out}e^{\phi_2}S_1L_1\sqrt{k_2D_2}}{(1+e^{2\phi_2})(S_1D_1+S_2L_1\sqrt{k_2D_2})-2S_1D_1} = \frac{2C_{out}e^{\phi_2}\Omega_{21}}{(1+e^{2\phi_2})(1+H_{21}\Omega_{21})-2} \quad (7)$$

$$C_2^{PR} = \frac{S_2}{S_1}C_1^{PR} = \frac{2C_{out}e^{\phi_2}S_2L_1\sqrt{k_2D_2}}{(1+e^{2\phi_2})(S_1D_1+S_2L_1\sqrt{k_2D_2})-2S_1D_1} = \frac{2C_{out}e^{\phi_2}H_{21}\Omega_{21}}{(1+e^{2\phi_2})(1+H_{21}\Omega_{21})-2} \quad (8)$$

where ϕ_2 denotes the initial Thiele modulus ϕ_{02} for the fully activated reactive layer 2 in the PR film, k_2 (= $\mu K_2 R_0$) is the initial apparent pseudo-first-order reaction rate in reactive layer 2; the solute partition coefficient H_{21} between the layers is

$$H_{21} = \frac{S_2}{S_1} = \frac{1}{H_{12}} \quad (9)$$

and the coupling parameter Ω_{21} is defined as

$$\Omega_{21} = L_1\frac{\sqrt{k_2D_2}}{D_1} = L_2\sqrt{\frac{k_2}{D_2}}\left[\frac{L_1}{D_1}\frac{D_2}{L_2}\right] = \frac{\phi_2}{\zeta_{1P2R}} \quad (10)$$

whereas the dimensionless parameter ζ_{1P2R} is a ratio of the kinetic transport properties of passive layer 1 to those of the passive matrix of reactive layer 2 (i.e., assumed to be containing inactive scavenger):

$$\zeta_{1P2R} = \left(\frac{D_1}{L_1}\right)_P \Big/ \left(\frac{D_2}{L_2}\right)_R \quad (11)$$

In the following discussions, the indices in the parameters ζ_{1R2P} and ζ_{1P2R} are dropped for convenience because the RP and PR film designs are discussed separately, and it is always clear which meaning of the parameter ζ is used. Note that ζ is always defined as ζ_{12}, that is, as a ratio of the passive transport properties of layer 1 to those of layer 2.

The interfacial concentrations $C_1(t)$ and $C_2(t)$ evolve as the reaction proceeds in the reactive layer and eventually result in the steady-state profiles of the solute through a passive–passive (PP) structure corresponding to complete exhaustion of the scavenger reactive capacity within the reactive layer. Then, these concentrations are found as

$$C_1^{PP} = \frac{1}{S_2}\times\frac{\frac{L_1}{D_1}C_{out}+\frac{L_2}{D_2}C_{in}}{\frac{L_1}{D_1S_1}+\frac{L_2}{D_2S_2}} = H_{12}\frac{C_{out}+\zeta C_{in}}{1+H_{12}\zeta} \quad (12)$$

$$C_2^{PP} = \frac{S_2}{S_1}C_1^{PP} = \frac{1}{S_1}\times\frac{\frac{L_1}{D_1}C_{out}+\frac{L_2}{D_2}C_{in}}{\frac{L_1}{D_1S_1}+\frac{L_2}{D_2S_2}} = \frac{C_{out}+\zeta C_{in}}{1+H_{12}\zeta} \quad (13)$$

Because the instantaneous solute equilibrium is always assumed to exist at the initial RP layer interface, C_2 is linearly related to C_1 through the partition coefficient H_{12} as defined in eq. (4). Hence, we only need to consider C_1 evolution as the solute scavenging reaction proceeds. Obviously the initial C_1^{RP} and C_1^{PR} differ from the final C_1^{PP} after the reaction is completed. Our analysis would be greatly simplified if it were possible to decouple solute diffusion and consumption dynamics within the reactive layer from the other layers. To do that, the fixed interfacial boundary conditions have to be imposed to continue the analysis within the SG model framework. To determine what kind of C_1 averaging between C_1^{RP} (or C_1^{PR}) and C_1^{PP} is necessary for that, we need to understand the evolution of C_1 as the reaction consuming the scavenger progresses in the reactive layer.

EVOLUTION OF INTERFACIAL CONCENTRATIONS IN THE RP FILM

With the steady–unsteady solution matching method developed in ref. 3, the instantaneous mass balance of the solute dissolved in the RP film at any reaction wavefront position $\{L_d = [L_1 \ldots 0]\}$ within the reactive layer 1 incorporated into the transient Thiele modulus (ϕ) of that layer (in the SG model sense) is described by the following system of linear equations:

$$\begin{cases} \beta_1+\beta_2 = a \\ \beta_1e^{\phi}+\beta_2e^{-\phi} = C_f \\ C_1 = H_{12}C_2 \\ (b-C_2)(\phi_0-\phi) = (C_1-C_f)\phi_0\zeta \\ C_1-C_f = (\phi_0-\phi)(\beta_1e^{\phi}-\beta_2e^{-\phi}) \end{cases} \quad (14)$$

where $a \equiv C_{in}$, where C_{in} is the equilibrium solute concentration within the inner membrane boundary; $b \equiv C_{out}$; C_f is the solute concentration in the moving reaction wavefront; ϕ_0 is the initial Thiele modulus ϕ_{01} of reactive layer 1; β_1 and β_2 are the coefficients in the steady-state solution of the reaction–diffusion equations for the permeant concentration in the catalytic reactive layer as determined from the boundary conditions; and C_f, C_1, C_2, β_1, and β_2 are the unknowns.

The first four equations in eq. (14) match the steady-state solute concentrations at all four interfaces, including the (slowly) propagating reaction wavefront (the fourth equation). The fifth equation matches the solute fluxes into and out of the wavefront at any position of the wavefront within the reactive layer. The solution of eq. (14) has the form

$$\delta_1 = (e^{2\phi} + 1)[1 - \phi + \phi_0(1 + H_{12}\zeta)] - 2 \quad (15)$$

$$C_f = \frac{1}{\delta_1}\{2ae^{\phi}[\phi_0(1 + H_{12}\zeta) - \phi] + bH_{12}(e^{2\phi} - 1)\} \quad (16)$$

$$C_1 = \frac{H_{12}}{\delta_1}\{2ae^{\phi}\phi_0\zeta + b[(e^{2\phi} + 1)(1 - \phi + \phi_0) - 2]\} \quad (17)$$

$$C_2 = \frac{1}{\delta_1}\{2ae^{\phi}\phi_0\zeta + b[(e^{2\phi} + 1)(1 - \phi + \phi_0) - 2]\} \quad (18)$$

$$\beta_1 = \frac{1}{\delta_1}[a(-1 - \phi + \phi_0 + H_{12}\phi_0\zeta) + bH_{12}e^{\phi}] \quad (19)$$

$$\beta_2 = \frac{1}{\delta_1}[ae^{2\phi}(1 - \phi + \phi_0 + H_{12}\phi_0\zeta) - bH_{12}e^{\phi}] \quad (20)$$

Equations (2) and (3) represent a special case of eqs. (17) and (18), respectively, at the moment of the scavenger activation ($t = 0$), namely, when $\phi = \phi_{01}$ and with the boundary condition $a = 0$. The choice of the boundary condition $C_{in} = 0$ is sufficient to avoid the situation when there is a solute flux into the reactive layer from the package contents with $p_{in} > 0$ during some finite time due to the noncatalytic scavenging reaction. In fact, as we established in ref. 2 for the homogeneous reactive layer, there is a critical solute concentration at the inner boundary ($C_{in.crit}$), below which the solute flux from the package into the reactive layer is not present at any time:

$$C_{in.crit} = C_{out}\text{sech}(\phi_0) \quad (21)$$

That translates into the ratio of the external solute pressures in the separated environments defining the boundary between unidirectional solute flow across the membrane ($p_{in} < p_{in.crit}$, where $p_{in.crit}$ is the critical pressure value inside the package) and bidirectional solute flow into the membrane ($p_{in} > p_{in.crit}$) for the catalytic scavenging reaction

$$\frac{p_{in.crit}}{p_{out}} = \text{sech}(\phi_0) \equiv \frac{2}{e^{\phi_0} + e^{-\phi_0}} \quad (22)$$

For the noncatalytic homogeneous scavenging reaction, the transient Thiele modulus ϕ_R of the reactive layer is gradually reduced as the reaction proceeds in the layer. Hence, instead of the initial ϕ_0 in eq. (22), as defined in eqs. (10) and (11) of part I, the transient Thiele modulus over the initial reactive layer thickness should be used to determine the transient critical solute pressure ratio:

$$\phi_R = \phi_R(t) = L\sqrt{\frac{\mu K}{D}\frac{1}{L}\int_0^L R(x, t)\,dx} \quad (23)$$

where R is the concentration of scavenger in the film material and x is a coordinate across the membrane thickness. This transient Thiele modulus is approximated in the SG model (ϕ_{SG}) by the modulus of only the remaining reactive part of the membrane in the presence of the slowly moving reaction wavefront completely consuming the scavenger and located at L_d:

$$\phi_{SG} = L_d(t)\sqrt{\frac{\mu K R_0}{D}} = \frac{L_d(t)}{L}\phi_0 \quad (24)$$

combined with the permeation through the passive (completely reacted) matrix with the thickness ($L - L_d$) left behind the front. The contribution to ϕ_R from the nearly exhausted (presumed to be passive) part of the membrane behind the wavefront in eq. (23) is the primary reason why eqs. (23) and (24) result in different values of ϕ_R and ϕ_{SG}. For example, the infinitely narrow wavefront located at $L_d = 0.5L$ will result in $\phi_R = \phi_0\sqrt{0.5}$ and $\phi_{SG} = 0.5\phi_0$. The difference is accounted for in the SG model when the coupling effect of the passive matrix behind the wavefront is considered and the definition [eq. (23)] is recovered in the limit of the narrow reaction wavefront. The wavefront movement coupled to permeation through the passive matrix leads to the evolution of the solute concentration at the moving RP interface, which results in eqs. (13) and (16) of part I. The net outcome of this process is that if the bidirectional solute flow into the membrane is initially present and the fixed boundary conditions are maintained, as the scavenging reaction proceeds within the layer, $p_{in.crit}$ will increase, which will eventually result in transition to the unidirectional flow pattern (when $p_{in.crit}$ exceeds the fixed p_{in} maintained inside the package). Now, we return to the analysis of the RP film where the reactive layer is described by the SG model, that is, itself as a RP structure with the moving interface.

For the RP film, $C_{in.crit}$ is determined from the condition of zero effective solute flux (J_0) across the boundary $x = 0$:

$$J_0 \equiv -D_1 \left.\frac{dC}{dx}\right|_{x=0} = 0 \tag{25}$$

Using the steady-state solution for the catalytic reactive membrane[2] where ϕ is constant:

$$C(\chi) = \beta_1 e^{\phi\chi} + \beta_2 e^{-\phi\chi} \tag{26}$$

$$\chi = \frac{x}{L} \tag{27}$$

(where χ is the dimensionless x coordinate) and substituting it into eq. (25) along with eqs. (19) and (20), we obtain for the noncatalytic RP film with moving reaction wavefront using ϕ_{SG}:

$$-J_0 = \sqrt{k_1 D_1}(\beta_1 - \beta_2) = \frac{\sqrt{k_1 D_1}}{\delta_1}\{-a[(e^{2\phi} - 1) \times (1 - \phi + \phi_0 + \phi_0 H_{12}\zeta) + 2] + 2bH_{12}e^{\phi}\} \tag{28}$$

In the following discussions, the transient Thiele modulus [$\phi = \phi(t)$] will always mean ϕ_{SG} as defined in eq. (24) by the SG model approximation of the remaining reactive layer thickness. Because δ_1 is always greater than zero and $k_1 = \mu K_1 R_0 > 0$, the condition of positive solute ingress into the package ($-J_0 > 0$) is transformed into

$$a(\phi) < \frac{2bH_{12}e^{\phi}}{(e^{2\phi} - 1)[1 - \phi + \phi_0(1 + H_{12}\zeta)] + 2} \tag{29}$$

In the RP film with a completely exhausted scavenger capacity in the reactive layer, that is, the PP film with $\phi = 0$, eq. (29) is reduced to

$$C_{in} < H_{12}C_{out} \tag{30}$$

which simply restates the fact that positive solute ingress into the package through the PP film is present when $p_{in} < p_{out}$. When the scavenger is at its full reactive capacity immediately after activation ($\phi = \phi_0$), eq. (29) limits the maximum solute concentration $a = C_{in}$ in the package to prevent solute reduction in the headspace due to the scavenging reaction

$$a(\phi_0) < \frac{2bH_{12}e^{\phi_0}}{(e^{2\phi_0} - 1)(1 + \phi_0 H_{12}\zeta) + 2} \tag{31}$$

The boundary between the two modes of permeation (involving solute ingress into the package and solute scavenging from the package headspace) can be expressed in terms of $C_{in.crit}$ as

$$\frac{C_{in.crit}}{C_{out}} = \frac{2H_{12}e^{\phi_0}}{(e^{2\phi_0} - 1)(1 + \phi_0 H_{12}\zeta) + 2} \tag{32}$$

Through the use of Henry's law for both exposed surfaces of the RP film, we obtain

$$C_{in} = S_1 p_{in} \tag{33}$$

$$C_{out} = S_2 p_{out} \tag{34}$$

and by applying eq. (32); $p_{in.crit}$ is found as follows:

$$\left.\frac{p_{in.crit}}{p_{out}}\right|_{t=0} = \frac{2e^{\phi_0}}{(e^{2\phi_0} - 1)(1 + \phi_0 H_{12}\zeta) + 2} \tag{35}$$

From the definition of permeance [steady-state transmission rate (TR)], $TR = P/L = DS/L$,[2,5] the complex $H_{12}\zeta$ is simply the ratio of solute permeances TR_1/TR_2 across the adjacent passive layers according to eqs. (4) and (6). Figure 2 demonstrates where in the dimensionless parameter space (ϕ_0, $H_{12}\zeta$) lie the boundaries separating the cases of unidirectional solute flux across the RP film driven by $\Delta p = p_{out} - p_{in}$ and bidirectional solute flux into the RP film from both adjacent environments caused by the scavenging reaction. According to eq. (31), all areas above the curves correspond to bidirectional flux into the film, and the areas below the curves correspond to unidirectional flux into the package.

Equation (35) describes only the effect of the initial Thiele modulus on the boundary between the unidirectional and bidirectional flow patterns. The approximate dynamics of this boundary in terms of the reduction in the transient Thiele modulus during the scavenging reaction can be inferred from eq. (29) as

$$\frac{p_{in.crit}(\phi)}{p_{out}} = \frac{2e^{\phi}}{(e^{2\phi} - 1)[1 - \phi + \phi_0(1 + H_{12}\zeta)] + 2} \tag{36}$$

This dynamics is shown in Figure 3. The x axis represents the reaction progress from 0 [fully activated reactive layer with $R(x) = R_0$ at $t = 0$] to 1 [completely deactivated reactive layer with $R(x) = 0$ in terms of the normalized reciprocal transient Thiele modulus: $\bar{\phi} = (1 - \phi/\phi_0)$]. The areas above the curves correspond to the bidirectional solute flow, that is, the scavenging of the solute from the package headspace in addition to the scavenging of the solute from the external environment. This effect has significant implications for active packaging practice because it proves that it is possible to remove or reduce the amount of oxygen trapped in the package with a suitable design of the reactive barrier structure. If, for example, the initially fixed solute pressure inside the package $p_{in} = 0.2p_{out}$, for a small ϕ_0 (=0.1), as shown in Figure 3(a), all the boundary curves lie above this fixed p_{in}. That means only the unidirectional flow (ingress) into the package will be present throughout the duration of the scavenging chemical reaction and obviously after its com-

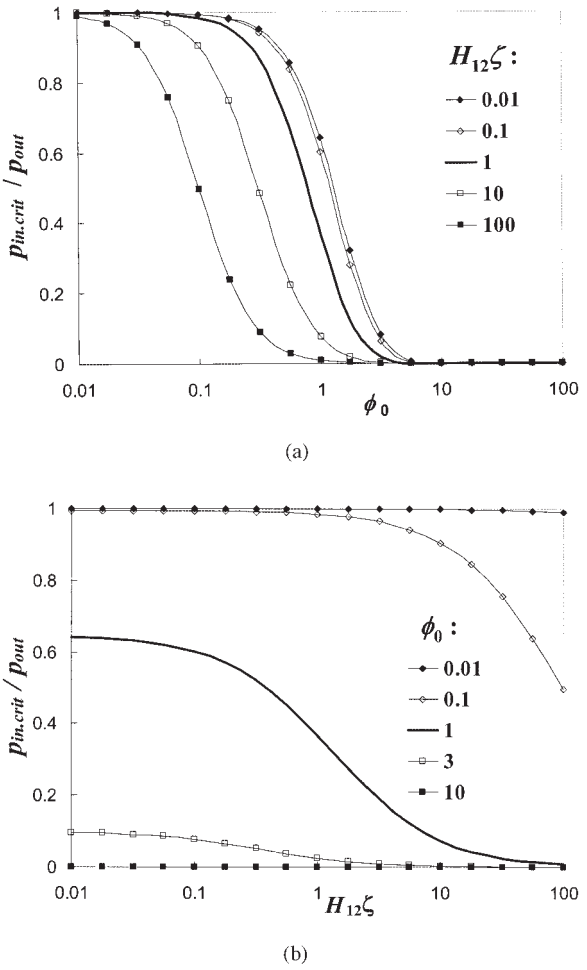

Figure 2 Dependence of the unidirectional–bidirectional permeation mode boundary on (a) ϕ_0 and (b) $H_{12}\zeta$.

pletion. On the other hand, for a larger ϕ_0 (=10), as shown in Figure 3(c), the bidirectional flow will exist during most of the reaction time (>95% in terms of transient Thiele modulus reduction dynamics). For the intermediate ϕ_0 (e.g., $\phi_0 = 1$), as shown in Figure 3(b), found to be important in some practical applications, the answer strongly depends on the ratio TR_1/TR_2 of the permeances of the individual passive layers (or the parameter combination $H_{12}\zeta$). When this ratio is smaller than or comparable with unity, meaning the reactive layer matrix provides most of or comparable barrier properties versus the passive layer protecting it from the environmental oxygen exposure, we get $p_{in} < p_{in.crit}$; hence, only the unidirectional flow into the package is present despite the reaction. On the other hand, when the reactive layer matrix provides negligible barrier to gas permeation versus the protective passive layer ($H_{12}\zeta \gg 1$), the bidirectional flow will be present throughout most of the reaction duration. For example, when $H_{12}\zeta = 100$, $p_{in.crit}$ will reach $p_{in} = 0.2p_{out}$ after approximately 96% of the reaction is completed (i.e., 96% of the scavenger reactive capacity is exhausted in the film), which will result in the transition from bidirectional to unidirectional flow at that time. For $H_{12}\zeta = 10$, this transition will take place earlier, after approximately 64% of the reaction is completed. Estimating the actual time to transition and the amount of the solute scavenged from the package

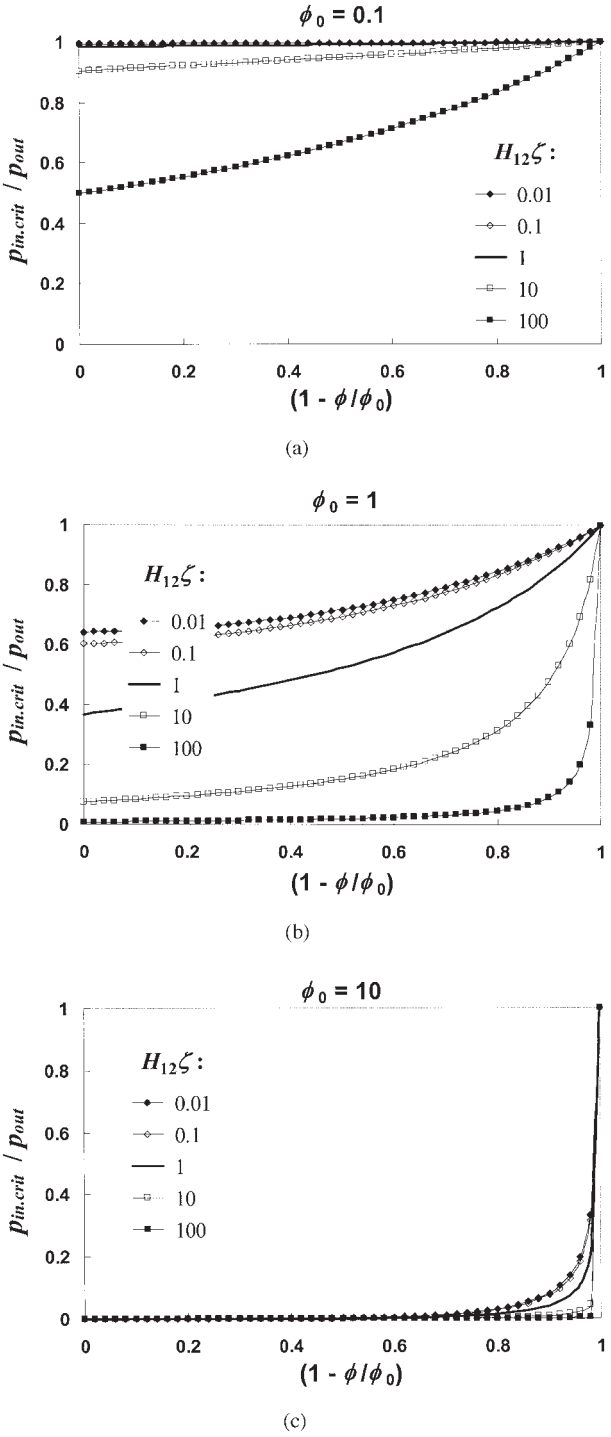

Figure 3 Dependence of the unidirectional–bidirectional permeation mode boundary on the transient Thiele modulus $\phi(t)$.

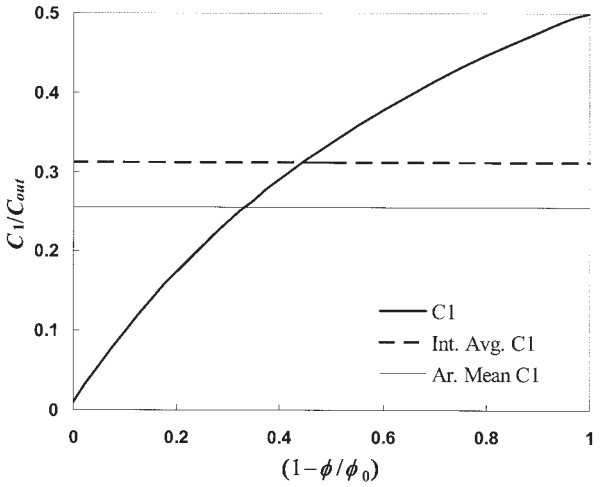

Figure 4 Evolution of C_1 in the RP film: $\phi_0 = 3.16$, $H_{12} = 1$, and $\zeta = 1$.

during that time is an interesting subject for further study, whereas here we focus on the unidirectional flow (ingress) analysis.

Figure 4 shows the evolution of the interfacial concentration (C_1) in the RP film according to eq. (17) as the noncatalytic scavenging reaction progresses within the reactive layer, reducing its transient Thiele modulus ϕ from ϕ_0 to 0. Even though $C_1(\phi)$ is nonlinear, the total change in C_1 is relatively small, and the integral average of $C_1(\phi)$ is close to the arithmetic mean of the initial and final interfacial concentrations for a wide range of control parameters ϕ_0, H_{12}, and ζ:

$$C_1^{IA} = \frac{1}{\phi_0}\int_0^{\phi_0} C_1(\phi)\, d\phi \approx \frac{C_1^{RP} + C_1^{PP}}{2} \qquad (37)$$

Figure 5 demonstrates this by the depiction of the error introduced by the arithmetic mean approximation [eq. (37)] for a wide range of control parameters (as percentage deviation of the integral average from the arithmetic mean, which is always positive in the RP film case). The deviation is acceptably small in most cases, except for large ϕ_0 and $H_{12}\zeta$ values close to 0.1. Even then, the error does not exceed 60%. Hence, we can choose this steady-state approximation as a representative fixed interfacial concentration for the analysis of the decoupled solute transport across the reactive and passive film layers:

$$C_1^* = \frac{C_1^{RP} + C_1^{PP}}{2} \qquad (38)$$

The validity of the approximation in eq. (38) must be further verified by numerical analysis, although our results indicate good agreement of the model with the numerical simulations. Figure 6 shows the effective flux dynamics and Figure 7 depicts the corresponding ingress dynamics for three representative initial Thiele moduli. The reason for the choice of parameter values $H_{12} = 1$ ($S_1 = S_2$) and $\zeta = 1$ (more specifically, $D_1 = D_2$ and $L_1 = L_2$) is that it allowed us to numerically integrate the original system of eqs. (1) and (2) of part I without complications. In general, the numerical solution of such systems is problematic because any deviation of H_{12} and ζ from unity results in a system of partial differential equations with discontinuous coefficients. It is possible to avoid the discontinuity caused by different S values of adjacent layers by the replacement of C in eqs. (1) and (2) of part I by p with Henry's law. The discontinuity caused by different D values of adjacent layers, however, cannot be eliminated by the redefinition of integration variables. That means that other approximate methods, such as the replacement of discontinuous diffusivities by continuous damping functions, have to be used. The power of the presented analytical approach is that all interfaces between dissimilar layers are treated explicitly with the assumption of instant equilibrium of the solute on both sides of the (infinitesimally narrow) interface. That allows us to predict the reaction–diffusion dynamics in very complex multilayer structures without resorting to numerical approximations.

The meaning of the error introduced by eq. (38) is that the ingress estimate overpredicted by the SG model approximation in eqs. (25) and (28) of part I will be reduced because of the positivity of this error. That is clearly seen in Figure 10(b,c) in part I, which shows the transient flux $J_0(t)$ slightly underpredicted by the SG model at the early stages of wavefront propagation. When the averaging error leads to a significant deviation from true behavior, as calculated in Figure 5 and shown in Figure 6(a,b), C_1^{IA} in eq. (37) should be used as a value of C_1^* instead of eq. (38). With eqs. (17) and (15), the integral average of $C_1(t)$ is expressed as

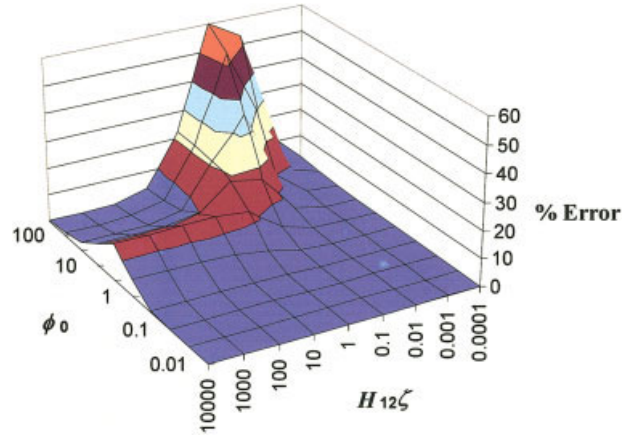

Figure 5 Deviation of C_1^{IA} from the arithmetic mean of its initial and final values. [Color figure can be viewed in the online issue, which is available at www.interscience.wiley.com.]

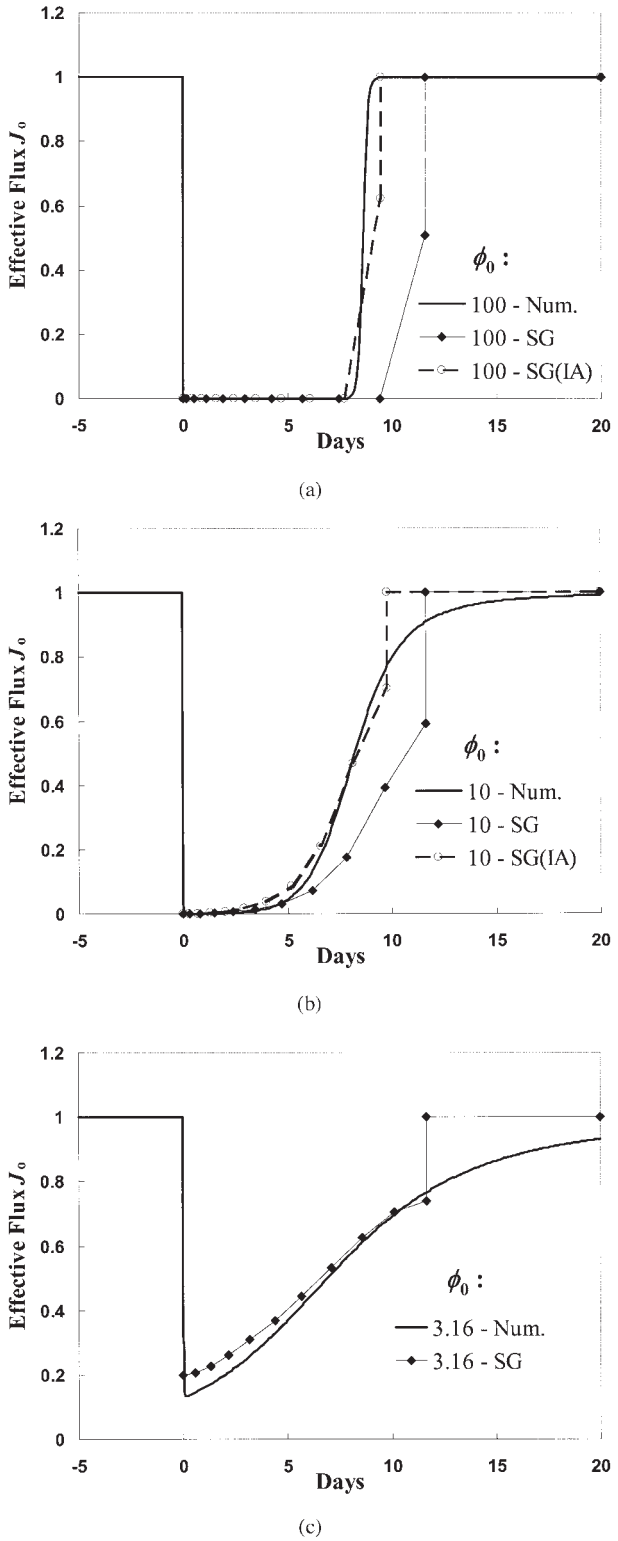

Figure 6 J_0 dynamics through the RP film with evolving (numerical) and fixed (SG model) interfacial concentrations: $H_{12} = 1$ and $\zeta = 1$.

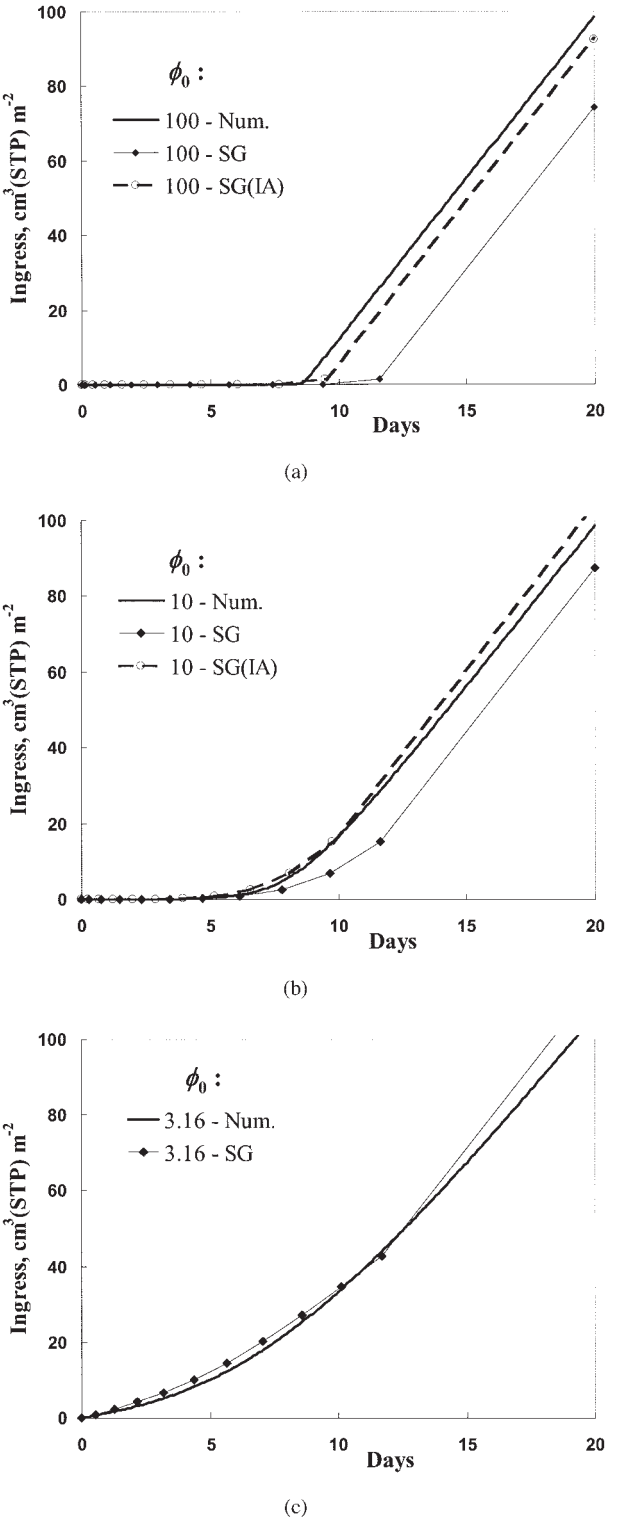

Figure 7 Solute ingress dynamics through the RP film with evolving (numerical) and fixed (SG model) interfacial concentrations: $H_{12} = 1$ and $\zeta = 1$.

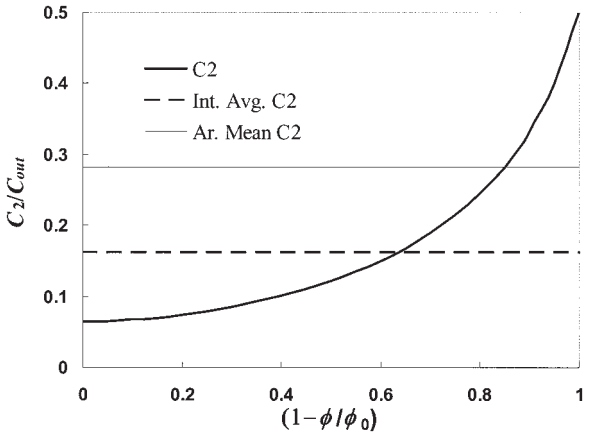

Figure 8 Evolution of C_2 in the PR film: $\phi_0 = 3.16$, $H_{12} = 1$, and $\zeta = 1$.

$$C_1^{IA} = \frac{1}{\phi_0} \int_0^{\phi_0} \frac{H_{12}\{2ae^{\phi}\phi_0\zeta + b[(e^{2\phi}+1)(1-\phi+\phi_0)-2]\}}{(e^{2\phi}+1)(1-\phi+\phi_0+\phi_0H_{12}\zeta)-2}\, d\phi \tag{39}$$

or as dimensionless ratio C_1^{IA}/C_{out} for the case $C_{\text{in}} = 0$:

$$\frac{C_1^{IA}}{C_{\text{out}}} = \frac{H_{12}}{\phi_0} \int_0^{\phi_0} \frac{(e^{2\phi}+1)(1-\phi+\phi_0)-2}{(e^{2\phi}+1)(1-\phi+\phi_0+\phi_0H_{12}\zeta)-2}\, d\phi \tag{40}$$

When a more accurate prediction of the ingress dynamics than the approximation in eq. (38) provides is required, eq. (40) can be evaluated numerically for specific cases of interest and C_1^{IA} can be used instead of C_1^*.

For sufficiently large ϕ_0 values, $C_1^{RP} \to 0$; hence, $C_1^* \approx C_1^{PP}/2$ can be used for the analysis of the RP film case instead of eq. (37). When the fixed boundary conditions are applied for each layer, the permeation dynamics through homogeneous reactive and passive layers can be resolved within the SG model framework.

EVOLUTION OF INTERFACIAL CONCENTRATIONS IN THE PR FILM

Analogous to the previous section, the following system of linear equations has to be solved for the solute mass balance in the PR film:

$$\begin{cases} \beta_1 + \beta_2 = C_2 \\ \beta_1 e^{\phi} + \beta_2 e^{-\phi} = C_f \\ C_1 = H_{12}C_2 \\ (C_1 - a)\zeta = (\beta_1 - \beta_2)\phi_0 \\ b - C_f = (\phi_0 - \phi)(\beta_1 e^{\phi} - \beta_2 e^{-\phi}) \end{cases} \tag{41}$$

where ϕ_0 and ϕ refer to the initial and transient Thiele moduli of reactive layer 2, respectively. In this case, the fourth and fifth equations in the system in eq. (41) match the solute fluxes out of and into both boundaries of the transient reactive layer, that is, the reactive sublayer of the initially fully reactive layer 2 within the SG model. The solution of eq. (41) has the form:

$$\delta_2 = e^{2\phi}(1-\phi+\phi_0)(\phi_0 + H_{12}\zeta) + (1+\phi-\phi_0)(\phi_0 - H_{12}\zeta) \tag{42}$$

$$C_f = \frac{1}{\delta_2}\{2ae^{\phi}(\phi_0-\phi)\zeta + b[(e^{2\phi}+1)(\phi_0+H_{12}\zeta) - 2H_{12}\zeta]\} \tag{43}$$

$$C_1 = \frac{H_{12}}{\delta_2}\{a\zeta[(e^{2\phi}+1)(\phi_0-\phi+1)-2] + 2be^{\phi}\phi_0\} \tag{44}$$

$$C_2 = \frac{1}{\delta_2}\{a\zeta[(e^{2\phi}+1)(\phi_0-\phi+1)-2] + 2be^{\phi}\phi_0\} \tag{45}$$

$$\beta_1 = \frac{1}{\delta_2}[a\zeta(\phi_0-\phi-1) + be^{\phi}(\phi_0+H_{12}\zeta)] \tag{46}$$

$$\beta_2 = \frac{1}{\delta_2}[ae^{2\phi}\zeta(\phi_0-\phi+1) + be^{\phi}(\phi_0-H_{12}\zeta)] \tag{47}$$

The transient effective flux across the PR film is equal to the flux across the inner boundary $x = L_1$ of reactive layer 2; that is, the dimensionless position of the reaction wavefront within the membrane $\xi = 0$ in the layer 2 coordinates:

$$-J_0 = \sqrt{k_2D_2}(\beta_1 - \beta_2) = \frac{\zeta\sqrt{k_2D_2}}{\delta_2}\{-a[(e^{2\phi}-1) \times (1-\phi+\phi_0)+2] + 2bH_{12}e^{\phi}\} \tag{48}$$

Because δ_2 is always greater than zero, the conditions of positive solute ingress into the package ($-J_0 > 0$) becomes [cf. eq. (29)]:

$$a(\phi) < \frac{2bH_{12}e^{\phi}}{(e^{2\phi}-1)(1-\phi+\phi_0)+2} \tag{49}$$

In a PR film with a completely depleted scavenger capacity in the reactive layer with $\phi = 0$ or essentially a PP film, the condition eq. (49) is again reduced to eq. (30), as expected. From eqs. (33) and (34), the initial boundary between the unidirectional and bidirectional flow patterns is

$$\left.\frac{p_{\text{in.crit}}}{p_{\text{out}}}\right|_{t=0} = \frac{2e^{\phi_0}}{e^{2\phi_0}+1} = \text{sech}(\phi_0) \tag{50}$$

That is, it is independent of the complex $H_{12}\zeta$, and it coincides with eq. (19) for the catalytic reactive single-layer membrane.

C_2 at the interfacial boundary of the reactive layer 2 will evolve as the reaction proceeds in the reactive layer. Figure 8 shows this evolution according to the extended SG model result [eq. (45)]. The steady-state approximation of C_2 may be chosen analogous to eq. (38) for the RP film:

$$C_2^{IA} = \frac{1}{\phi_0}\int_0^{\phi_0} C_2(\phi)\, d\phi \left(\approx \frac{C_2^{PR}+C_2^{PP}}{2} \,? \right) \tag{51}$$

$$C_2^{*} = \frac{C_2^{PR}+C_2^{PP}}{2} \tag{52}$$

Figure 9(a,b) shows the error in C_2 introduced by the fixed arithmetic mean approximation in eq. (52), again as a percentage deviation of the integral average from the arithmetic mean. The deviation is always negative and, in absolute terms, is often larger than that of eq. (37) for the RP film. Comparing Figure 9 for the PR film to Figure 5 for the RP film, we observe that the error of approximation eq. (52) for the PR film is sensitive to the values of the individual parameters H_{12} and ζ rather than the complex $H_{12}\zeta$. For the practically important cases of $\phi_0 > 2$, which can also be reliably handled by the SG model, we conclude that approximation in eq. (52) is valid only for very large values of ζ (>1000). In other cases, the use eq. (52) will lead to overestimation of the ingress through the PR film. As we recall from the ζ definition in eq. (11) for the PR film, a large ζ means the passive layer provides negligible passive barrier compared to that of the reactive layer matrix. This case has no practical importance because such situations can be well described by the SG model results for the single-layer reactive film.

To correct the error introduced by eq. (52), let us consider the evolution of C_2 for the initial Thiele moduli of interest: $\phi_0 > 2$. Figure 10 confirms that for larger ϕ_0 (>10), the interfacial concentration is well approximated by $C_2(t) = 0$ during most of the reaction progress except the final stages near scavenger capacity exhaustion. When ϕ_0 is not that large, that is, comparable to 2, we can try to further reduce the error in the averaging approximation by choosing

$$C_2^{*} = C_2^{PR} \tag{53}$$

This approximation will preserve the inequality

$$C_2^{*} < C_2^{IA} \tag{54}$$

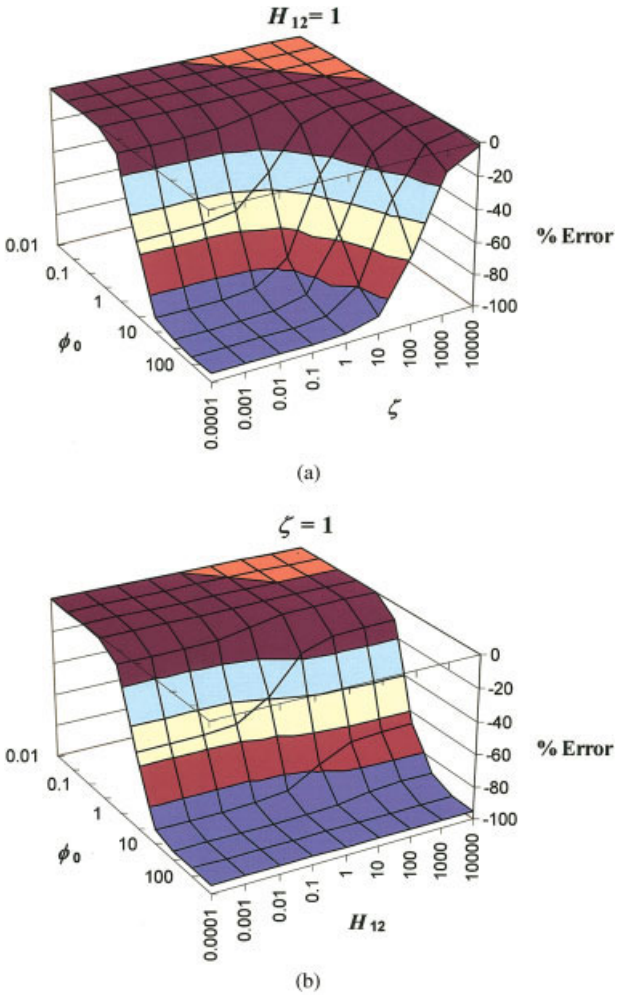

Figure 9 Deviation of C_2^{IA} from the arithmetic mean of its initial and final values: (a) $H_{12} = 1$ and (b) $\zeta = 1$. [Color figure can be viewed in the online issue, which is available at www.interscience.wiley.com.]

resulting in underprediction of the (steady-state) flux at the solute exit boundary $x = 0$ and overprediction of the transient flux into the passive layer at the initial PR interface $x = L_1$. Hence, eqs. (52) and eq. (53) fail to represent the ingress dynamics through the PR film and are unacceptable for its analysis. It is also apparent from Figures 8–10 that no single fixed C_2 approximation will be able to represent true system behavior unless ϕ_0 of the reactive layer 2 is close to zero. Next, we introduce a new method of resolving this problem for intermediate ϕ_0 values based on the SG model solutions for the reactive film and dynamic ingress scaling arguments.

METHOD OF INGRESS ANALYSIS THROUGH THE PR FILM

Let us consider the reactive film and PR film, where the reactive layer has the same properties (thickness,

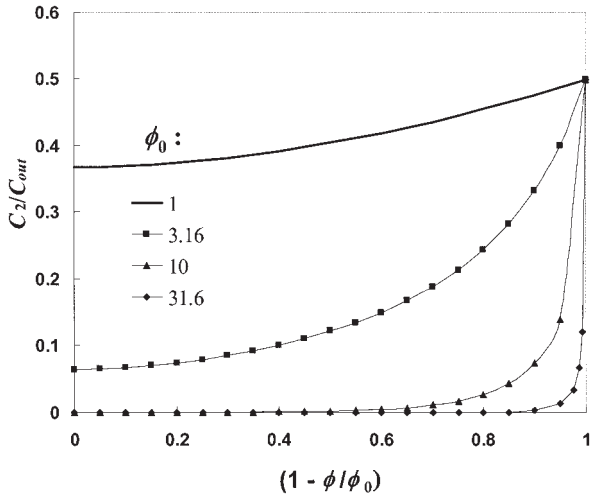

Figure 10 Evolution of C_2 in the PR film as a function of the initial Thiele modulus.

matrix material, scavenger, amount, dispersion, and activation mechanism) in both films and both films are exposed to the same environments and activated at the same time. The properties of the passive layer in the PR film are arbitrary except for the requirement of material homogeneity and uniform layer thickness. We apply the same semipermeable narrow reaction wavefront concept as originally suggested by the SG model in refs. 3 and 4 to analyze both films. In case of the PR film, it means that despite the evolution of $C_2(t)$, which is not equal to zero as $C_{in} = 0$ originally assumed in the reactive film analysis, any solute permeating ahead of the wavefront is not consumed by the reaction and does not reduce the scavenging reactive capacity of the yet unreacted sublayer in the reactive layer. Even though $C_2(t) > 0$, the boundary condition $C_{in} = 0$ prevents the formation of the second reaction wavefront propagating from the PR interface into the reactive layer, that is, against the external solute concentration gradient as discussed in ref. 3. As a result, we conclude that within the semipermeable reaction wavefront framework, the SG model time of scavenger capacity exhaustion (t_E°) will be the same in both the reactive and PR films when both reactive layers (in the reactive and PR films) are exactly the same:

$$t_E^\circ(R) = t_E^\circ(PR) \tag{55}$$

where R indicates the reactive layer. Moreover, we postulate that the dynamics of solute permeation through both reactive layers will be the same because it is largely driven by the reaction wavefront dynamics, that is, by the solute diffusion from the p_{out} environment coupled with its consumption by the sufficiently fast reaction, rather than by the solute concentration gradient dC/dx across the membrane. However, $J_0(t)$ will be different for these films because the presence of the passive layer in the PR film will create additional resistance to the permeation of the solute that penetrated ahead of the semipermeable reaction wavefront. These fluxes are easily found at time $t = 0$ of scavenger activation and time $t = t_E^\circ$ of scavenger exhaustion with the SG model. From eq. (13) of part I, we have for the reactive film at $t = 0$

$$-J_0^R(0) = \frac{DC_{out}}{L}\,\phi_0 \mathrm{sech}(\phi_0) \tag{56}$$

and from eq. (23) of part I for the P film at $t \geq t_E^\circ$

$$-J_0^R(t_E^\circ) = -J_x^P = \frac{DC_{out}}{L} \tag{57}$$

To correlate eqs. (56) and (57) with the PR film analysis, the reactive film properties D and L should correspond to the reactive layer properties D_2 and L_2 in the PR film. As noted earlier, the SG model works only for systems with diffusion-controlled reactions where $\phi_0 > 2$; hence, eq. (56) cannot be used to predict the transition from reactive flux to passive flux [eq. (57)] in the limit of activation-controlled reactions as $\phi_0 \to 0$.

For the PR film we have from eq. (48) at $t = 0$

$$-J_0^{PR}(0) = \frac{\zeta\sqrt{k_2 D_2}}{\delta_2}\left[-a(e^{2\phi_0} + 1) + 2bH_{12}e^{\phi_0}\right] \tag{58}$$

After one assumes $C_{in} \equiv a = 0$ and with eq. (42) to find δ_2, the final expression for the initial effective flux through the PR film is

$$-J_0^{PR}(0) = \frac{D_2 C_{out}}{L_2}\frac{2\phi_0 H_{12}\zeta}{e^{\phi_0}(\phi_0 + H_{12}\zeta) + e^{-\phi_0}(\phi_0 - H_{12}\zeta)} \tag{59}$$

For the PR film at $t \geq t_E^\circ$ we use the PP film result [eq. (13)] with $C_{in} = 0$:

$$-J_0^{PR}(t_E^\circ) = -J_x^{PP} = \frac{D_2(C_{out} - C_2^{PP})}{L_2} = \frac{D_2 C_{out}}{L_2}\frac{H_{12}\zeta}{1 + H_{12}\zeta} \tag{60}$$

Figure 11(a,b) shows examples of the effective flux dynamics through the reactive and PR films with two initial and two final fluxes marked and flux dynamics linearized between the scavenger activation and exhaustion times. One should not conclude from Figure 11 that such linearization is a sound approach: Figure 4 in part I and Figure 11(b) in this part clearly demonstrate that for larger initial Thiele moduli, the flux dynamics is highly nonlinear; hence, the linearization procedure is unlikely to yield acceptable results. Our

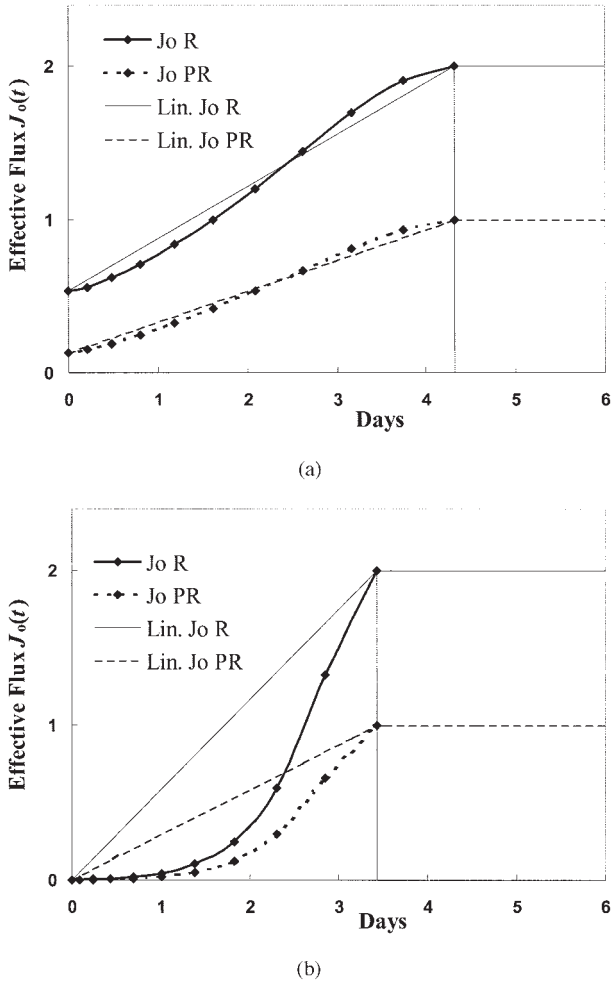

Figure 11 $J_0(t)$ dynamics through reactive and PR films: $H_{12} = 1$, $\zeta = 1$, and $\phi_0 =$ (a) 3.16 and (b) 10.

intention is to calculate the difference between the solute ingress [eq. (29) of part I] through the reactive film during the scavenger exhaustion time and the ingress obtained by linearization of the effective flux. That difference can then be scaled in time to the linearized ingress and applied to the linearized flux dynamics through the PR film. Namely, the linearized ingress through the reactive (I_R^L) film is found from eqs. (56) and (57) as

$$I_R^L(t_E^\circ) = \frac{J_0^R(0) + J_0^R(t_E^\circ)}{2}\, t_E^\circ \tag{61}$$

whereas eq. (29) of part I gives an estimate of the actual ingress (I_R^+) during the same time. Then, the relative correction factor (Δ_R) can be defined as the solution of the equation

$$I_R^+ = I_R^L + \Delta_R I_R^L \tag{62}$$

that has a form

$$\Delta_R = \frac{I_R^+}{I_R^L} - 1 \tag{63}$$

If we postulate that Δ_R represents the ingress correction to the value of I_{PR}^L through the PR film during t_E° (this is the assumption of dynamic scalability of the PR film ingress due to additional diffusion resistance of the passive layer 1), the ingress with nonlinear flux dynamics is found analogously to eq. (62) as

$$I_{PR}^+ = I_{PR}^L + \Delta_R I_{PR}^L \tag{64}$$

or as

$$I_{PR}^+ = I_R^+ \frac{I_{PR}^L}{I_R^L} \tag{65}$$

In eqs. (64) and (65), I_{PR}^L is found analogously to eq. (61) as

$$I_{PR}^L(t_E^\circ) = \frac{J_0^{PR}(0) + J_0^{PR}(t_E^\circ)}{2}\, t_E^\circ \tag{66}$$

Combining eqs. (61), (66), and (65), we obtain for the Δ_R-corrected $I_{PR}^+(t_E^\circ)$

$$I_{PR}^+(t_E^\circ) = I_R^+(t_E^\circ)\, \frac{J_0^{PR}(0) + J_0^{PR}(t_E^\circ)}{J_0^R(0) + J_0^R(t_E^\circ)} \tag{67}$$

Equation (67), along with eq. (29) of part I and eqs. (56), (57), (59), and (60) of this part, form the ingress analysis tool for the PR films. Figure 12 compares the J_0 dynamics obtained by numerical integration with the dynamics predicted by the SG model when eq. (67) was applied to the SG model of transient ingress [eq. (28) of part I] through the reactive film in part I. Good agreement of the extended SG model results with the numerical simulations was observed.

PRACTICAL IMPLICATIONS

Although the deviation of the SG model predictions from the numerical results increases as ϕ_0 is reduced, that is, as diffusion control of the overall reaction rate is weakened, it is worth noting that in the PR film case, the extended SG model consistently overpredicts the transient ingress. Thus, the proposed model provides an upper estimate of the ingress that serves as a safety margin for a packaging engineer designing a multilayer RP structure. On the other hand, models based on the impermeable wavefront hypothesis, such as the Yang–Nuxoll–Cussler (YNC) model[6] and its analogues[7] formally derived in the asymptotic infinite time limit always underpredict the transient ingress during any finite timescale. This underprediction becomes significant as ϕ_0 of the reactive layer is reduced,

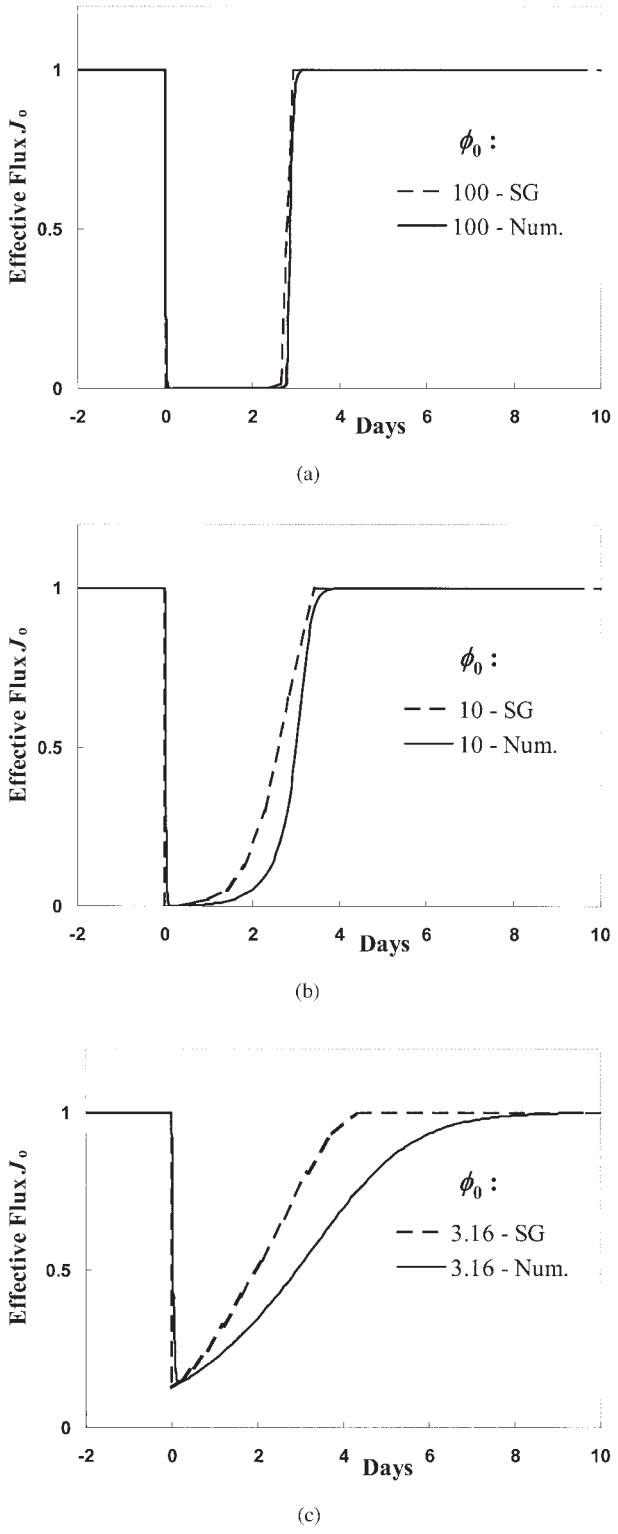

Figure 12 Comparison of transient flux dynamics in the PR film obtained by numerical simulations with the SG model predictions: $H_{12} = 1$, $\zeta = 1$, and $\phi_0 =$ (a) 100, (b) 10, and (c) 3.16.

potentially resulting in incorrect design decisions. The extended SG model does not have such a disadvantage and allows an engineer to test the scavenger containing multilayer designs with confidence.

CONCLUSIONS

In part II of this series, we introduced the analysis methodology for scavenger consumption dynamics and solute ingress through the RP and PR structures with noncatalytic solute scavenging reaction in the reactive layer. This methodology is based on the original SG model of transient permeation that we developed.[2–4] With the framework for the transient ingress analysis established for the RP and PR films, in part III of the series, we will analyze specific cases of two-layer RP barriers, introduce generalized solutions for multilayer films, and provide a practical guide to optimized design of RP barrier structures.

NOMENCLATURE

Additional relevant nomenclature is included in parts I and III of this series of articles.

C_1 solute concentration at the layer 1 side of the interface between layers 1 and 2

C_1^* the fixed Solovyov–Goldman model approximation of the transient interfacial concentration C_1

C_1^{IA} integral averaged solute concentration at the layer 1 side of the interface

C_2 solute concentration at the layer 2 side of the interface between layers 1 and 2

C_f solute concentration in the reaction wavefront moving across the reactive layer

D_1 solute diffusivity in layer 1 of a multilayer film (m^2/s)

D_2 solute diffusivity in layer 2 of a multilayer film (m^2/s)

J^{PP} steady-state solute flux through a two-layer passive barrier [cm^3 (STP) m^{-2} s^{-1}]

k_1 initial apparent pseudo-first-order reaction rate in reactive layer 1 ($= \mu K_1 R_0$; s^{-1})

k_2 initial apparent pseudo-first-order reaction rate in reactive layer 2 ($= \mu K_2 R_0$; s^{-1})

L_1 thickness of layer 1 (m)

L_2 thickness of layer 2 (m)

S_1 solubility coefficient of a particular solute in the layer 1 matrix [cm^3 (STP) m^{-3} Pa^{-1}]

S_2 solubility coefficient of particular solute in the layer 2 matrix [cm^3 (STP) m^{-3} Pa^{-1}]

Greek symbols

β_1, β_2 coefficients in steady-state solution of reaction–diffusion equations for permeant concentration in catalytic reactive layer (determined from the boundary conditions; mol/m^3)

χ dimensionless x coordinate ($= x/L$))

Δ_R relative correction factor for calculation of the solute ingress through a reactive layer with nonlinear flux dynamics with linearized ingress analysis

$\bar{\phi}$ normalized reciprocal transient Thiele modulus in the Solovyov–Goldman model sense

ϕ_1 initial Thiele modulus of noncatalytic reactive layer 1 in the RP film

ϕ_2 initial Thiele modulus of noncatalytic reactive layer 2 in the PR film

ζ relative passive mass transport parameter for two adjacent layers

References

1. Solovyov, S. E.; Goldman, A. Y. J Appl Polym Sci 2006, 100, 1940.
2. Solovyov, S. E.; Goldman, A. Y. Int J Polym Mater 2005, 54, 71.
3. Solovyov, S. E.; Goldman, A. Y. Int J Polym Mater 2005, 54, 93.
4. Solovyov, S. E.; Goldman, A. Y. Int J Polym Mater 2005, 54, 117.
5. Crank, J. The Mathematics of Diffusion, 2nd ed.; Clarendon: Oxford, 1975.
6. Yang, C.; Nuxoll, E. E.; Cussler, E. L. AIChE J 2001, 47, 295.
7. Siegel, R. A.; Cussler, E. L. J Membr Sci 2004, 229, 33.